25. OSCILLATIONS AND WAVES IN A MODEL OF $InsP_3$-CONTROLLED CALCIUM DYNAMICS

Hans G. Othmer and Yuanhua Tang

Department of Mathematics
University of Utah
Salt Lake City, UT 84112

25.1 INTRODUCTION

Various types of cells use changes in intracellular calcium triggered by hormones, neurotransmitters or growth factors as a second messenger to trigger a variety of intracellular responses, including contraction, secretion, growth and differentiation. One of the earliest experiments that revealed the complexity of the calcium response is that due to Woods *et al.* (1986), who studied the response of hepatocytes to vasopressin, a hormone that mobilizes intracellular calcium. They found that over the range of 200 nM to 1 μM in the hormone concentration, stimuli evoke repetitive spikes in the intracellular calcium concentration, rather than simply elevating the level of calcium. Moreover, they found that as the hormone concentration was raised, the frequency of spiking increased, but the amplitude remained nearly constant. Thus the continuously-graded (analog) extracellular hormone signal was converted into a frequency-encoded digital signal (the number of calcium spikes). Similar dynamic behavior has been found in a large number of cell types since then, and has lead to the suggestion that calcium spiking and frequency encoding must have a physiological role. Since high calcium levels are cytotoxic, it is necessary to maintain a low average concentration of calcium, but since calcium frequently serves primarily as a trigger for other processes, a transient elevation above a low mean concentration suffices for this purpose. Moreover, using a large transient increase as the trigger permits the use of a sharper threshold for response, and hence better noise discrimination. Other possible advantages are suggested by Meyer & Stryer (1991), but to date there is little hard evidence that the spiking plays an essential physiological role.

Of potentially greater significance is the fact that the response in many cells is also spatially inhomogeneous. In a variety of cell types, waves of calcium release propagate across the cell in response to hormonal or other stimuli. For instance, in *Xenopus laevis* oocytes, penetration of a sperm into the egg triggers a localized increase in cytosolic calcium that propagates away from the point of entry at approximately 10 μ/sec, inducing cortical contraction, meiosis, and structural rearrangement (Gilkey *et al.* 1978; Nuccitelli 1991). In addition, there is evidence that at least some of the hormone-sensitive calcium stores in *Xenopus* oocytes are localized at the animal pole (Lupu-Meiri *et al.* 1988; Berridge 1990), and thus in either fertilization or hormonal stimulation, propagation of the wave is essential for inducing the entire cell to respond to a localized stimulus. In hepatocytes the oscillations

Experimental and Theorietcal Advances in Biological Pattern Formation,
Edited by H.G. Othmer *et al.*, Plenum Press, New York, 1993

appear to originate from a single locus and propagate across the cell. Moreover, the initiation site seems to be relatively constant in a given cell, even for different agonists. Thus when hepatocytes are treated with phenylephrine, followed by washout and restimulation with vasopressin, Ca^{+2} waves originate from the same site. The speed of the waves in hepatocytes is typically 20-25 μ/sec. These cells are polarized to a degree and a variety of receptors are known to be concentrated at the sinusoidal membrane, which may account for the origin of the wave. Finally, spatial variations in calcium are important at the supracellular level as well. For instance, calcium waves may be used to synchronize large cell assemblies such as ciliated epithelial cells (Meyer 1991), and diffusion of inositol 1,4,5–trisphosphate ($InsP_3$) through gap junctions appears to be necessary for the propagation of these waves (Boitano *et al.* 1992).

In cardiac and smooth muscle cells, calcium is sequestered primarily in the sarcoplasmic reticulum, whereas in cells that are not electrically excitable it is stored in the endoplasmic reticulum. Calcium in the sarcoplasmic reticulum is bound to a high-affinity protein called sequestrin, which is thought to reside in organelles called calciomes. Wong *et al.* (1992) have developed a model for calcium-induced calcium release (CICR) from the SR. In non-excitable cells at least part of the sequestered calcium can usually be released by binding of $InsP_3$ to a receptor that controls the permeability of a calcium channel in the ER membrane. This channel is a tetramer which can open to four distinct conductance levels that are multiples of a unit step of 20 pS (Watras *et al.* 1991). $InsP_3$ binding is obligatory for opening of the channel (Harootunian *et al.* 1991), as is calcium (Watras *et al.* 1991). Low calcium levels promote opening of the channels, while high levels inhibit opening (Finch *et al.* 1991; Bezprozvanny *et al.* 1991).

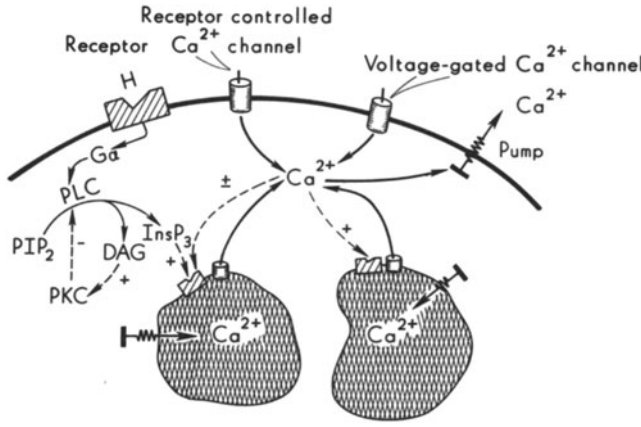

Figure 25.1. A schematic of the transduction system for hormonal stimuli, the calcium transport mechanisms, and the $InsP_3$-sensitive and $InsP_3$-insensitive stores. Key: G_α: The G protein that activates phospholipase C (PLC); PIP_2: phosphatidylinositol 4,5-bisphosphate; $InsP_3$: inositol 1,4,5-trisphosphate; DAG: diacylglycerol; PKC: protein kinase C. Solid lines indicate a material flow, and dashed lines indicate a control influence.

A typical sequence for transduction of an agonist signal into a variation in intracellular calcium is as follows (*cf.* Figure 25.1). The agonist binds to a plasma membrane receptor and the complex catalyzes the GDP/GTP exchange in a G protein. The G_α component in turn activates phospholipase C, the enzyme that catalyzes the hydrolysis of phosphatidylinositol 4,5-bisphosphate to $InsP_3$ and diacylglycerol. $InsP_3$ then binds to an $InsP_3$ receptor that is

part of the calcium channel complex on the ER membrane, and if calcium is also bound at the calcium-activating site the channel opens. Frequently, sequestered calcium in cells that are not electrically-excitable can also be released, either from the $InsP_3$-sensitive store or from a distinct store, through another type of calcium channel that is $InsP_3$-insensitive. For instance, Thomas *et al.* (1991) cite evidence that in hepatocytes only 30-50% of the non-mitochondrial calcium is released from the $InsP_3$-sensitive pool, even when the calcium pump is inhibited; the remainder is released by calcium ionophores. In Figure 25.1 we indicate that these stores are distinct, but that is not known in general.

Under prolonged hormonal stimulation, or when $InsP_3$ is injected directly into the cell, calcium spiking occurs only in a range of hormonal or $InsP_3$ concentrations (DeLisle *et al.* 1990). Rooney *et al.* (1989) found that there was a correlation between the latent period and the subsequent oscillation period over a range of agonist doses and oscillation frequencies. In hepatocytes the shape of the oscillations depends on the agonist. The rate of rise of the calcium transient is more-or-less independent of the agonist, but the declining phase is highly dependent on the agonist. For example, phenylephrine-induced transients decay much more rapidly than do the transients induced by vasopressin. Thomas *et al.* (1991) cite evidence that protein kinase C may be involved in the re-uptake.

Extracellular calcium is needed in hepatocytes to sustain the calcium oscillations: in its absence the frequency of oscillation is reduced and the oscillations eventually run down. However in larger cells such as oocytes, the major features of the observed dynamics are not dependent on the presence of extracellular calcium or calcium-induced calcium release from intracellular stores. Consequently, in this paper we focus on a model in which there is no calcium transport between the interior and the exterior of the cell, and no calcium-induced calcium release; the oscillations center on the dynamics of the $InsP_3$ receptor. Our objective is to develop a model that is complex enough to reproduce the major aspects of the experimental observations, yet which is simple enough to be analyzed qualitatively in order to understand how the component processes affect the overall dynamics. The major assumptions of the model are that calcium binds to the activating site on the channel only after $InsP_3$ has bound to the receptor, and that the binding of calcium to the inhibitory site occurs only after calcium is bound to the activating site. This assumption of sequential binding leads to a model with only a few states that lends itself to qualitative analysis of the effect of various parameters. As we shall see later, the oscillations arise from the biphasic response of the $InsP_3$-sensitive calcium channel to calcium.

An outline of the remainder of the paper is as follows. In the following section we briefly review some of the previous models for calcium dynamics. In Section 25.3 we introduce a simple two-state receptor model and show analytically that under very general conditions this scheme cannot produce oscillations. We then introduce a four-state model, and in Section 25.4 we show that this model correctly reproduces the experimentally-observed bell-shaped response of the activated channel to calcium. We also show how excitability arises in this scheme, we demonstrate that it produces oscillations over a range of $InsP_3$ levels, and we show that these oscillations show frequency coding as a function of the $InsP_3$ level. Finally, in Section 25.5 we illustrate some of the wave phenomena that are possible in this model.

25.2 AN OVERVIEW OF MODELS FOR CALCIUM DYNAMICS

Calcium oscillations will in general involve many intracellular components, but in order to understand which components are essential and which are not, it is helpful to

identify major subsystems and determine how they are involved in the overall process. One can identify three major subsystems in Figure 25.1, (i) the transduction subsystem whereby hormonal signals are transduced via G-proteins into an $InsP_3$ signal, (ii) a system comprising the $InsP_3$-sensitive calcium store, and (iii), a system comprising an $InsP_3$-insensitive calcium store, which may include voltage- and receptor-gated membrane channels. Of course not all cells will necessarily have all of these components.

Given this subdivision, one can identify a number of distinct ways in which calcium oscillations can be generated. Firstly, the transduction system may generate an oscillatory $InsP_3$ signal in response to a constant hormonal stimulus. This could arise from a feedback loop in which DAG activates protein kinase C, which in turn phosphorylates the G-protein that couples the receptor to phospholipase C, thereby leading to a reduction in the production of $InsP_3$ and DAG, which would reduce the inhibition of transduction, and so on. We call this a type I oscillator, and the model proposed by Cobbold *et al.* (1991) is of this type. This type produces an oscillatory input into the $InsP_3$-sensitive calcium subsystem, and in such systems the $InsP_3$ oscillations drive the calcium oscillations.

In a second class of models the oscillations are generated within the $InsP_3$-sensitive calcium store subsystem. As we remarked earlier, it is known that in a number of systems the $InsP_3$-sensitive calcium channel is not activated unless calcium occupies an activating site on the receptor. Furthermore, the channel conductivity is reduced at high calcium concentrations, probably due to the presence of a calcium-binding inhibitory site on the receptor. The model proposed by De Young & Keizer (1992); Keizer & De Young (1992) and the model we propose later incorporate these observations. In both these models $InsP_3$ is treated as a parameter; oscillations in the cytosol calcium arise without any temporal variation in the level of $InsP_3$. As we show later, such a system is excitable in the usual sense that there is a threshold level of the $InsP_3$ stimulus below which there is no significant response, but above which there is a large response. As frequently happens in such systems, tuning the system parameters slightly produces oscillatory behavior. In our model $InsP_3$ is both the stimulus that produces an excitable response, and the parameter which produces oscillatory behavior in a suitable range. This is in accord with the experimental observations, in that injection of $InsP_3$ can produce either single calcium transients or calcium oscillations, depending on the stimulus level (Dupont *et al.* 1991).

In a third class of models the oscillations are confined within the calcium subsystem. Since these do not involve transduction of hormonal stimuli, except as they involve modulation of calcium channels in the plasma membrane, they will not be treated here.

In addition to the three pure types described above, there are a variety of mixed types, in which there are feedforward or feedback interactions between two or more of the subsystems described above. For example, the model of Meyer & Stryer (1988) involves cooperative release of calcium from the $InsP_3$-sensitive store, coupled with Ca^{+2} activation of PLC. Thus the transduction subsystem and the $InsP_3$-sensitive store are mutually coupled, and oscillations arise from the feedback interaction between these two subsystems. A model due to Berridge and co-workers (Goldbeter *et al.* 1990), which is conceptually similar to a model proposed by Kuba & Takeshita. (1981), involves both an $InsP_3$-sensitive calcium store and an $InsP_3$-insensitive store. In this model $InsP_3$ is also a parameter, not a dynamic variable. A more complicated model, in which the transduction subsystem is linked to calcium dynamics has been proposed by Cuthbertson & Chay (1991).

25.3 THE MATHEMATICAL MODEL

25.3.1 Two states for the IP3 receptor do not suffice

Our interest is in systems in which a steady calcium input into the cytoplasm, either from the extracellular space or an internal pool, is not essential for generating the oscillations. In the absence of such inputs the total amount of intracellular calcium is conserved if there is no transport out of the cell, and it follows that a two-variable model in which the only dynamic variables are the concentrations of calcium in the cytosol and in the active storage compartment cannot give rise to oscillations, whether or not $InsP_3$ plays a role in the release of calcium. This applies, in particular, to the model of Goldbeter *et al.* (1990), and to that of Somogyi & Stucki (1991). It is conceivable however, that a model in which the $InsP_3$ receptor has two distinct states may give rise to oscillation. However we show in this section that oscillations cannot arise in response to hormonal stimulation in such a model under very mild restrictions on the functional form of the receptor response to $InsP_3$ and calcium. This leads us to a more complex four state model that we describe later in this section and analyze in the following section.

Suppose that the receptor can exist in one of two states, and that transitions between these states occur according to the first-order scheme

$$R \underset{k_{-1}}{\overset{k_1}{\rightleftarrows}} R^*. \tag{25.1}$$

To incorporate the $InsP_3$ binding to the bare receptor R, as well as the activating and inhibitory effects of calcium, we suppose that

$$k_1 = k_{10} f_0(I, C), \tag{25.2}$$

where I and C are the concentrations of $InsP_3$ and cytosol calcium, respectively. The function f_0 should be monotone increasing in I, monotone increasing in C at low C, and monotone decreasing in C at high C. In addition to the calcium flux through the $InsP_3$-sensitive channel, we suppose that there is a basal calcium leakage between the store and the cytosol, and a pump from the cytosol into the store (*cf.* Figure 25.1). Finally, we suppose that the conductivity of the $InsP_3$-sensitive channel is an increasing function of the fraction of receptors in the state R^*. Let z denote the fraction of receptors in the state R^*; then the governing equations for C and z can be written

$$\begin{aligned} \frac{dC}{dt} &= (1 + v_r)(\gamma_0 + \gamma_1 f(z))(C_0 - C) - \bar{g}(C) \\ \frac{dz}{dt} &= k_{10} f_0(I, C)(1 - z) - k_{-1} z. \end{aligned} \tag{25.3}$$

Here γ_0 is the basal permeability of the ER (which includes the channel conductance in the absence of $InsP_3$), and γ_1 is the density of $InsP_3$-sensitive channels per unit volume of ER. The function $f(z)$ represents the dependence of the channel conductivity on the fraction of channels in the conducting state RIC^+, and we assume that $f' \geq 0$. C_0 is the volume-average intracellular calcium concentration, which is defined by the relation

$$C_0 = \frac{C + v_r C_s}{1 + v_r},$$

where v_r is the ratio of the ER volume to the cytosol volume and C_s is the calcium concentration in the store. The function $\bar{g}$ represents the active pump, and thus $\bar{g}(C) \geq 0$ and $\bar{g}'(C) \geq 0$. It is necessary that $C \geq 0$, and that $z \in [0,1]$, and it is easy to see that the set $\Omega \equiv \{(C,z) \mid C \geq 0$ and $z \in [0,1]\}$ is invariant under the flow of (25.3).

The stable steady state of the system at low values of $InsP_3$ should correspond to low values of cytosol calcium, and we wish to determine whether this can be destabilized and lead to oscillations at a critical value of $InsP_3$. Thus consider the Jacobian of (25.3) at a steady state (C^*, z^*), which is the matrix

$$K = \begin{bmatrix} -(1+v_r)(\gamma_0 + \gamma_1 f(z^*)) - \bar{g}'(C^*) & (1+v_r)\gamma_1 f'(z^*)(C_0 - C^*) \\ k_{10}\dfrac{\partial f_0}{\partial C}(I, C^*)(1-z^*) & -k_{10} f_0(I, C^*) - k_{-1} \end{bmatrix}.$$

In order to destabilize the system to growing oscillations (*i. e.* in order to produce a Hopf bifurcation) as I is increased, the sum of the diagonal terms must vanish, whereas the off-diagonal terms must have opposite signs. However, neither of these conditions can be met under the stipulated conditions on the functions f_0, f and g. Thus the steady state cannot be destabilized by increasing the hormone concentration, and hence the $InsP_3$ concentration, and we conclude that under the forgoing conditions, a single-pool, $InsP_3$-gated model with two receptor states cannot undergo a Hopf bifurcation. In fact one can prove that the system can never oscillate, but this will not be done here. Thus we must incorporate more receptor states, and we next introduce a scheme with four states that can produce oscillations. One can show that a three-state version of this model can also oscillate, but the dynamic behavior possible is limited.

25.3.2 A four-state single pool model

We suppose that the receptor has four states, and that the transitions between them occur according to the following scheme.

$$\begin{aligned} I + R &\underset{k_{-1}}{\overset{k_1}{\rightleftarrows}} RI \\ RI + C &\underset{k_{-2}}{\overset{k_2}{\rightleftarrows}} RIC^+ \\ RIC^+ + C &\underset{k_{-3}}{\overset{k_3}{\rightleftarrows}} RIC^+C^- \end{aligned} \tag{25.4}$$

As before, R denotes the bare receptor, I denotes $InsP_3$ and C denotes the cytosol calcium concentration. Further, RI denotes the receptor-$InsP_3$ complex, and RIC^+ (respectively, RIC^+C^-) denotes RI with calcium bound at the activating site (respectively, the activating and inhibitory sites). In addition, there is calcium diffusion between the calcium store and the cytoplasm, and a calcium pump between the cytosol and the calcium store. At present I is treated as a parameter.

Let $x_i, i = 2, \ldots 5$, denote the fractions in states R, RI, RIC^+ and RIC^+C^-, respectively. Then the governing equations are

$$\begin{aligned} \frac{dC}{dt} &= (1+v_r)(\gamma_0 + \gamma_1 f(x_4))(C_0 - C) - \bar{g}(C) \\ \frac{dx_2}{dt} &= -k_1 I x_2 + k_{-1} x_3 \end{aligned}$$

$$\begin{aligned}
\frac{dx_3}{dt} &= -(k_{-1} + \bar{k}_2 C)x_3 + k_1 I x_2 + k_{-2} x_4 \qquad (25.5)\\
\frac{dx_4}{dt} &= -(k_{-2} + \bar{k}_3 C)x_4 + \bar{k}_2 C x_3 + k_{-3} x_5\\
\frac{dx_5}{dt} &= \bar{k}_3 C x_4 - k_{-3} x_5. \qquad (25.6)
\end{aligned}$$

We suppose that $f(x) = x$, *i. e.* that the channel conductivity is a linear function of the fraction of channels open. The calcium pump between the cytoplasm and the ER is known to be a tetramer with four calcium binding sites, and therefore we assume that

$$\bar{g}(C) = \frac{\bar{p}_1 C^4}{C^4 + \bar{p}_2{}^4}.$$

We define $x_1 = C/C_0$, and after eliminating x_5 by use of the conservation condition $\sum_{k=2}^{5} x_k = 1$, we can write the governing equations in the form

$$\begin{aligned}
\frac{dx_1}{dt} &= \lambda(\gamma_0 + \gamma_1 x_4)(1 - x_1) - \frac{p_1 x_1^4}{p_2^4 + x_1^4}\\
\frac{dx_2}{dt} &= -k_1 I x_2 + k_{-1} x_3\\
\frac{dx_3}{dt} &= -(k_{-1} + k_2 x_1)x_3 + k_1 I x_2 + k_{-2} x_4 \qquad (25.7)\\
\frac{dx_4}{dt} &= k_{-3} - k_{-3} x_2 + (k_2 x_1 - k_{-3})x_3 - (k_{-2} + k_3 x_1 + k_{-3})x_4,
\end{aligned}$$

where $\lambda \equiv 1 + v_r$, $k_2 = \bar{k}_2 C_0$, $k_3 = \bar{k}_3 C_0$, $p_1 = \bar{p}_1/C_0$, and $p_2 = \bar{p}_2/C_0$. In this scaling all x_i range between 0 and 1, and it is easy to see that the set $\{x_i \mid 0 \le x_i \le 1\}$ is invariant under the flow of (25.7). As we show in Section 25.4, this scheme is sufficiently robust to reproduce many of the observations.

25.3.3 Parameter values

In this section we give the values of parameters in the four-state model that are used in later simulations and give the rationale for their choice.

The ratio of the ER volume to the cytoplasmic volume v_r is taken to be 0.185, after Alberts *et al.* (1989). The leakage rate between the calcium store and cytoplasm is known to be small. We use the value $\gamma_0 = 0.1 s^{-1}$, but the value of this parameter does not significantly influence the dynamics as long as it is small.

The average calcium concentration is taken as $C_0 = 1.56 \mu M$. This leads to a maximal calcium concentration in the ER (with zero calcium concentration in the cytoplasm) of $10 \mu M$, which is in the physiological range (De Young & Keizer 1992).

Joseph *et al.* (1989) report that the dissociation constant for $InsP_3$ binding to microsomal ER fractions in the absence of calcium is approximately $0.15 \mu M$. We choose $k_1 = 12.0(\mu M \cdot s)^{-1}$ and $k_{-1} = 8.0 s^{-1}$, which gives $K_1 = 0.15 \mu M$.

There are no experimental data on the kinetic constants of calcium binding to the channels. We choose the set of values of k_2, k_{-2}, k_3, and k_{-3} given in Table 25.1 so as to make activation a much faster process compared to the binding of calcium to the inhibitory site. This set of data also provides an adequate fit to the bell-shaped channel opening curve in response to calcium changes and the saturation curve for the channel opening in response to $InsP_3$ increases.

Table 25.1. Parameter values for the four-state model

Parameter	Value	Parameter	Value
v_r	0.185	k_1	$12.0\,(\mu M \cdot s)^{-1}$
γ_0	$0.1s^{-1}$	k_2	$15.0\,(\mu M \cdot s)^{-1}$
γ_1	$20.5s^{-1}$	k_3	$1.8\,(\mu M \cdot s)^{-1}$
$\bar{p}_1$	$8.5\,(\mu M \cdot s)^{-1}$	k_{-1}	$8.0s^{-1}$
$\bar{p}_2$	$0.5\mu M$	k_{-2}	$1.65s^{-1}$
C_0	$1.56\mu M$	k_{-3}	$0.21s^{-1}$

γ_1 is a parameter that incorporates both the effect of calcium channel density and the channel conductance. Although the channel conductance is known for cerebellum cells (Watras *et al.* 1991), the channel concentration is not reported there. However, the value of γ_1 we use is consistent with that conductance and the channel densities reported for other cells. The calcium pumping parameters $\bar{p}_1$ and $\bar{p}_2$ are also unknown. We choose them, as well as the remaining kinetic constants, so as to qualitatively reproduce the following experimental results.

- In the absence of $InsP_3$, the equilibrium Ca^{2+} concentration in the cytoplasm should be of the order of $50nM$ (*cf.* Figure 25.4).
- The K_d for $InsP_3$ binding to the channel increases to about $0.5\mu M$ in the presence of $1\mu M$ calcium (Joseph *et al.* 1989).
- The Ca^{2+} oscillations should occur in a reasonable range of $InsP_3$ concentration and the system should be excitable for $InsP_3$ below this range.
- When the $InsP_3$ concentration is in the range that produces oscillations, the system should exhibit frequency coding.

The parameter values are listed in Table 25.1. The corresponding parameters needed for the nondimensional equations can easily be calculated from these values.

25.4 ANALYSIS OF THE LOCAL DYNAMICS IN THE FOUR-STATE MODEL

25.4.1 Steady-state analysis

From the steady-state version of (25.7) we find that

$$\begin{aligned} x_3 &= (\frac{k_1 I}{k_{-1}})x_2 && \equiv K_1^{-1}x_2 \\ x_4 &= (\frac{k_2 x_1}{k_{-2}})x_3 && \equiv K_2^{-1}x_1 x_3 \\ x_2 &= \frac{K_1 K_2}{K_2(K_1+1)+x_1+K_3 x_1^2} \end{aligned}$$

where $K_3 \equiv k_3/k_{-3}$. Therefore the fractions in the states RI and RIC^+ are given by

$$x_3 = \frac{K_2}{K_2(K_1+1)+x_1+K_3 x_1^2} \tag{25.8}$$

$$x_4 = \frac{x_1}{K_2(K_1+1)+x_1+K_3x_1^2} \equiv X_4(x_1), \tag{25.9}$$

The $InsP_3$ dependence of these fractions enters through K_1, and it follows that $x_i \to 0$, $i = 2,3,4$, as $InsP_3 \to 0$, as they should. Furthermore, $x_4 \to 0$ as $x_1 \to 0$.

Since the fractions in the various receptor states at steady state can be expressed in terms of the dimensionless calcium concentration, these fractions can be computed knowing the solution of the scalar equation

$$\lambda(\gamma_0+\gamma_1x_4)(1-x_1) = \frac{p_1x_1^4}{p_2^4+x_1^4}, \tag{25.10}$$

where x_4 is given by (25.9). Before analyzing this equation we consider the case in which calcium is clamped, as in the experiments by Bezprozvanny *et al.* (1991).

It follows from (25.9) that the fraction of channels open at a fixed calcium concentration increases with the calcium concentration at low concentrations and decreases at high concentrations. One finds that the maximum open fraction occurs at the dimensionless calcium concentration

$$x_1^* = \sqrt{\frac{K_2(K_1+1)}{K_3}},$$

and that the fraction open at this value is

$$x_4^* = \frac{1}{1+\sqrt{K_2K_3(K_1+1)}}.$$

Since $K_1 = k_{-1}/k_1I$, the maximum increases as $\sqrt{I}$ for small I. The width of the graph of $X_4(x_1)$ at half the maximal open fraction is determined by the roots of the equation

$$\frac{1}{2}x_4^* = X_4(x_1),$$

from which one finds that the half-width is

$$\begin{aligned}\Delta x_1 \equiv x_1^+ - x_1^- &= \frac{\sqrt{4-2x_4^*+(1-4K_3K_2(K_1+1))(x_4^*)^2}}{K_3x_4^*} \\ &= \frac{\sqrt{3\left(1+2\sqrt{K_2K_3(K_1+1)}\right)}}{K_3}\end{aligned}$$

Thus the half-width is very weakly dependent on the $InsP_3$ concentration. The graph of $X_4(x_1)$ is shown in Figure 25.2(a), and the experimentally-derived curve is shown in Figure 25.2(b). Certainly the model parameters could be tuned to reproduce the experimental results as well as desired, but because there is no complete set of data available for the system from which Figure 25.2 is obtained, we have not done this.

Now consider the steady state Equation (25.10), which reads

$$\lambda\left(\gamma_0+\frac{\gamma_1x_1}{K_3x_1^2+x_1+K_2(K_1+1)}\right)(1-x_1) = \frac{p_1x_1^4}{p_2^4+x_1^4}. \tag{25.11}$$

The left-hand side of (25.11) has the value $\lambda\gamma_0$ at $x_1 = 0$, it vanishes at $x_1 = 1$, and has a unique minimum in (0,1). On the other hand, the right-hand side vanishes at $x_1 = 0$, is monotone increasing in x_1, and attains its half-maximal value at $x_1 = K_4$. Depending on the

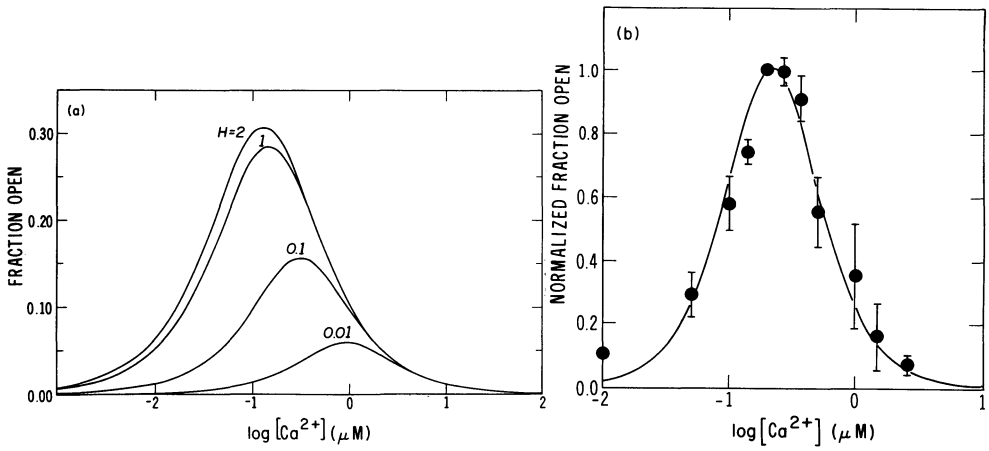

Figure 25.2. (a) The theoretically-predicted graph of the fraction of activated channels as a function of cytosol calcium. (b) The experimentally-measured curve for $InsP_3 = 2.0\mu M$ (from Bezprozvanny *et al.* 1991.)

choice of parameters, there may be one or three steady states at a fixed $InsP_3$ concentration. However, if K_4 is chosen sufficiently large there is a unique positive steady state for all values of I. It is easy to show that the steady-state calcium concentration is a monotone increasing function of I. It then follows from (25.9) that the fraction of channels open at the steady state is monotone increasing in I provided that the steady state level of calcium is such that $x_1 < x_1^*$ for all $I \in (0, \infty)$. A plot of the fraction open computed for the standard parameters is shown in Figure 25.3(a), and the experimentally-observed curve for cerebellar cells is shown in Figure 25.3(b). One can formally compute $\partial x_1/\partial I$ from (25.9) and (25.10) to determine the asymptotic dependence of the fraction open on $InsP_3$, but the results are too complex to be useful in the range of interest. However, one finds numerically that the theoretical curve given in Figure 25.3(a) can be fit moderately well using a Hill function in $InsP_3$ with an exponent of 1.75. Experimental values of the Hill coefficient for $InsP_3$-induced calcium release range from 1.0-1.3 (Volpe *et al.* 1990) to greater than 3.7 (Delisle 1991).

25.4.2 Excitability and Oscillations

As we observed earlier, the experimentally-observed dynamics of the $InsP_3$-triggered calcium release have the hallmarks of a classical excitable system as the phrase is used, for example, in the context of nerve conduction equations (Alexander *et al.* 1990; Othmer 1991). To understand the origin of excitability in this system it is helpful to represent the kinetic mechanism schematically as follows.

$$R \underset{8}{\overset{12}{\rightleftarrows}} RI \underset{1.65}{\overset{15}{\rightleftarrows}} RIC^+ \underset{0.21}{\overset{1.8}{\rightleftarrows}} RIC^+C^- \tag{25.12}$$

The first forward reaction involves binding of $InsP_3$, while the last two forward reactions involve binding of calcium. The numerical values of the rate constants are indicated, and from these one sees that binding of calcium to the activating site is an order of magnitude faster than binding of calcium to the inhibitory site at all concentrations. Similarly, $InsP_3$ binding is fast as long as $InsP_3$ is $\geq \mathcal{O}(0.1)$.

There are two aspects of excitability that are of interest here: (i) the response to pulses of $InsP_3$ and (ii), the response to a pulse of calcium in a system with fixed $InsP_3$. We

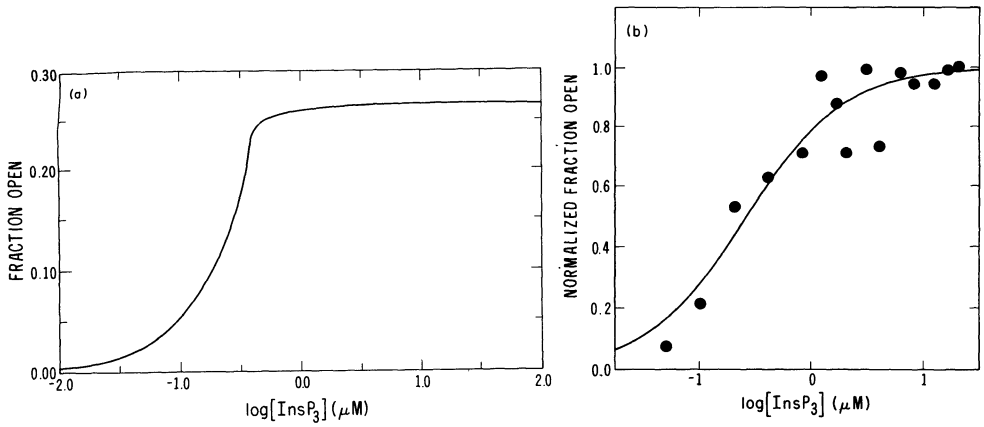

Figure 25.3. (a) The theoretically-predicted fraction of channels open as a function of the $InsP_3$ concentration. In this figure the calcium is not clamped, but rather, is obtained from the solution of the full set of steady state equations. (b) The experimentally-measured curve for cerebellar cells. 100% corresponds to 14% open. (From Watras *et al.* 1991)

consider the former case first. In the absence of $InsP_3$, $x_2 = 1$, $x_i = 0, i = 3,4,5$, and the calcium concentration is low. If a step change in $InsP_3$ is made, $InsP_3$ binds rapidly with R, and calcium rapidly binds with the RI complex at the activating site. Since RIC^+ opens the calcium channels, the cytosol calcium increases, which in turn produces more activated receptor. Thus the initial rapid response only involves $x_1, \cdots x_4$, and one of the receptor fractions can be eliminated by the conservation condition. More precisely, if one rescales the full system (25.5) and makes use of the difference in kinetic coefficients in (25.12) to eliminate x_5, and if one uses the conservation condition to eliminate x_2, then one arrives at the system

$$\begin{aligned} \frac{dx_1}{dt} &= \lambda(\gamma_0 + \gamma_1 x_4)(1 - x_1) - \frac{p_1 x_1^4}{p_2^4 + x_1^4} \\ \frac{dx_3}{dt} &= -(k_{-1} + k_2 x_1 + k_1 I)x_3 + (k_{-2} + k_1 I)x_4 + k_1 I \\ \frac{dx_4}{dt} &= k_2 x_1 x_3 - (k_{-2} + k_3 x_1)x_4. \end{aligned} \tag{25.13}$$

On the surface $\dot{x_3} = 0$ one has

$$x_3 = \frac{k_1 I + (k_{-2} - k_1 I)x_4}{k_{-1} + k_2 x_1 + k_1 I}. \tag{25.14}$$

Therefore, on the intersection of $\dot{x_4} = 0$ with this surface one has that

$$x_4 = \frac{k_1 k_2 x_1 I}{k_{-1}k_{-2} + k_3 x_1(k_2 + k_{-1}) + k_1 I(k_{-2} + k_3 + k_2 x_1)} \tag{25.15}$$

Similarly, on $\dot{x_1} = 0$ one has

$$x_4 = \left(\frac{g(x_1)}{\lambda(1 - x_1)} - \gamma_0\right)/\gamma_1. \tag{25.16}$$

In Figure 25.4(a) we show the intersections of the null surfaces $\dot{x_1} = 0$ and $\dot{x_4} = 0$ with the null surface $\dot{x_3} = 0$, projected into the $x_1 - x_4$ plane. One sees from (25.15) that on

$\dot{x}_4 = 0$, x_4 is an increasing function of x_1, while on $\dot{x}_1 = 0$, x_4 is independent of x_1. It is easy to see that depending on the value of I, there may be one or three steady states in the fast dynamics. For instance, when $I = 0.36$ there are three, and the significance of this value will become clear later. In Figure 25.4(a) we also show the x_1 and x_4 components of the full system (25.5), starting at the steady state for $I = 0$, and applying a square-wave stimulus of amplitude $I = 0.36$ and duration either 3 or 4 seconds. One sees there that a 3-second stimulus is subthreshold, while a 4-second stimulus is superthreshold. It is clear in that figure that the unstable manifold of the intermediate steady state of the fast system, which is a saddle point, serves as a threshold, and stimuli which carry the state above this manifold produce a significant amplification of cytosol calcium, while stimuli that leave the state below this manifold can be termed subthreshold. The time course of the calcium component of the response for the foregoing stimuli is shown in Figure 25.4(b), and these illustrate that this system is excitable in the sense used in Othmer (1991).

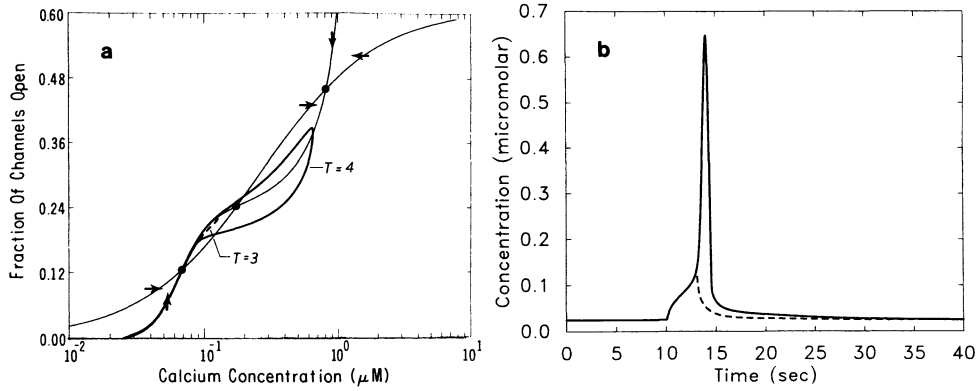

Figure 25.4. (a) The intersection of the null surfaces $\dot{x}_1 = 0$ and $\dot{x}_4 = 0$ with the null surface $\dot{x}_3 = 0$, projected into the $x_1 - x_4$ plane. The dashed curve represents the response of a system at steady state with $I = 0$ to a square-wave impulse in $InsP_3$ of amplitude $I = 0.36$ and of 3 seconds duration, and the heavy solid curve is the response to a 4 second stimulus of the same duration. (b) The time course of the calcium component for these stimuli.

The response for an $InsP_3$ stimulus of fixed duration and varying amplitude is shown in Figure 25.5. This figure also shows that the latency in the response is inversely-related to the amplitude of the stimulus, as is observed experimentally. It is clear that one could compute the threshold stimulation for a variety of amplitude-duration pairs and thereby construct an amplitude-duration curve for this excitable system, but this is not done here. A similar analysis can be done to understand excitability with respect to calcium perturbations at fixed $InsP_3$. In this case we freeze x_5 at its steady-state value for the given value of $InsP_3$ and analyze the fast dynamics as before. In Figure 25.6(a) we show the time course of calcium and in Figure 25.6(b) the time course of the fraction of open channels for two initial perturbations in calcium. It is clear from these figures that a sufficiently large pulse triggers an excitable response, and in view of this, one expects that these dynamics can generate propagating calcium waves when $InsP_3$ is spatially-uniform and a spatially-localized perturbation of calcium is introduced. It should be noted in Figure 25.6(a) that the initial pulse triggers a secondary response, which is what is observed experimentally when REF2 cells that are treated with vasopressin are exposed to a calcium pulse (Harootunian *et al.* 1991). In the experimental context the secondary response is broad (*cf.* Figure 2(b) in Harootunian *et al.* (1991)), but this is the result of cell-to-cell differences in the population.

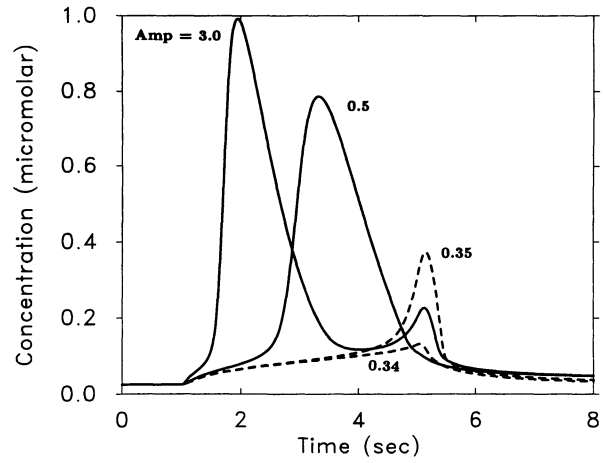

Figure 25.5. The response of a system at steady state to a square-wave stimulus in $InsP_3$ of 4 seconds duration and of the amplitude indicated on the figure. Note that a sufficiently large stimulus generates a secondary response that coincides time-wise with the response generated to a stimulus of smaller amplitude.

As I is increased, one finds that oscillations set in at $I \sim 0.366$ and persist until $I \sim 2.57$. We show the amplitude of the calcium component of the periodic solution in this range in Figure 25.7. It should be noted that the maximum amplitude of the oscillations decreases somewhat over the oscillatory range of $InsP_3$, but the period changes by an order of magnitude. Thus the system exhibits the experimentally-observed frequency coding. In Figure 25.8 we show the calcium concentration and the conducting channels at $I = 0.4$, which is in the oscillatory regime. Note that there are two phases in the early part of each cycle, a phase in which calcium rises slowly and the fraction of channels open begins to rise, followed by a phase in which the channels open very rapidly and calcium rises rapidly.

In the preceding figures the concentration of $InsP_3$ has been held fixed. However, under normal circumstances $InsP_3$ is degraded, and thus the foregoing results only strictly apply when a non-hydrolyzable analog of $InsP_3$ is used. However, it is clear that if $InsP_3$ is degraded, and if the initial concentration is larger than the upper limit of the oscillatory range of $InsP_3$, then as $InsP_3$ decreases the system sweeps through the entire range of oscillatory dynamics. The details of the dynamics will of course depend on the rate at which $InsP_3$ is degraded. By controlling the $InsP_3$ level experimentally one can control the passage through various dynamical regimes. This is illustrated in Figure 25.9(a), where we show the calcium concentration as a function of time when the time course of $InsP_3$ is as given in the figure caption. The experimentally-observed behavior for endothelial cells under the same stimulus protocol (albeit on a different time scale) is shown in Figure 25.8(b), which is reproduced from R. Jacob, J. E. Merritt & Rink (1988).

25.5 WAVES

One of the most striking aspects of calcium dynamics in oocytes is the wide variety of wave patterns that are observed (Lechleiter *et al.* 1991; Lechleiter & Clapham 1992). A model based on calcium-induced calcium release that can qualitatively reproduce these observations is proposed in Girard *et al.* (1992). This model uses the model of Goldbeter *et al.* (1990)

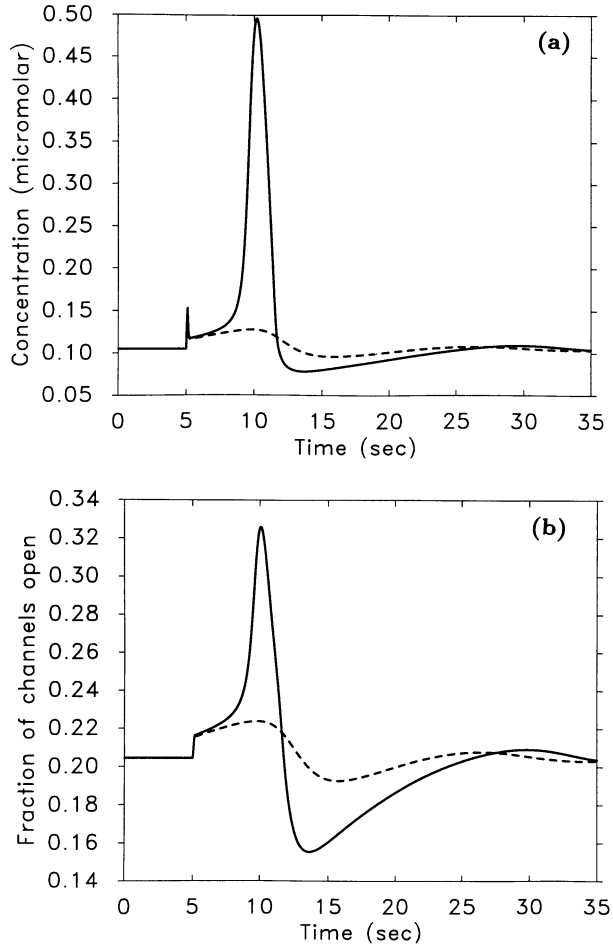

Figure 25.6. The time course of calcium (a) and the fraction of open channels (b). The system is in a steady state for fixed $I = 0.36$ when $T \in (0, 5)$, and a square wave of calcium of amplitude 1.2 (solid lines) or amplitude 1.15 (dashed lines) is imposed for 0.1 second at $T = 5$.

for the local dynamics. However, as we noted earlier, calcium transport across the plasma membrane plays an essential role in this model, yet the major features of the calcium dynamics in oocytes do not depend on this, at least on a short time scale. Furthermore, it is known that there are no ryanodine receptors, and therefore there is no $InsP_3$-insensitive calcium pool, in *Xenopus* oocytes (D. Clapham, personal communication). In hamster eggs the $InsP_3$-sensitive pool plays an essential role in the calcium waves, for when the eggs are treated with antibodies to the $InsP_3$ receptor, the waves are blocked (Miyazaki *et al.* 1992).

In this section we briefly describe some of the wave patterns that are predicted by the $InsP_3$-controlled model developed here. We include diffusion of both calcium and $InsP_3$, and therefore the governing equations in a spatially distributed system are as follows.

$$\begin{aligned} \frac{\partial x_1}{\partial t} &= D_{CA}\Delta x_1 + \lambda(\gamma_0 + \gamma_1 x_4)(1 - x_1) - \frac{p_1 x_1^4}{p_2^4 + x_1^4} \\ \frac{\partial y}{\partial t} &= D_I \Delta y + H - y \end{aligned}$$

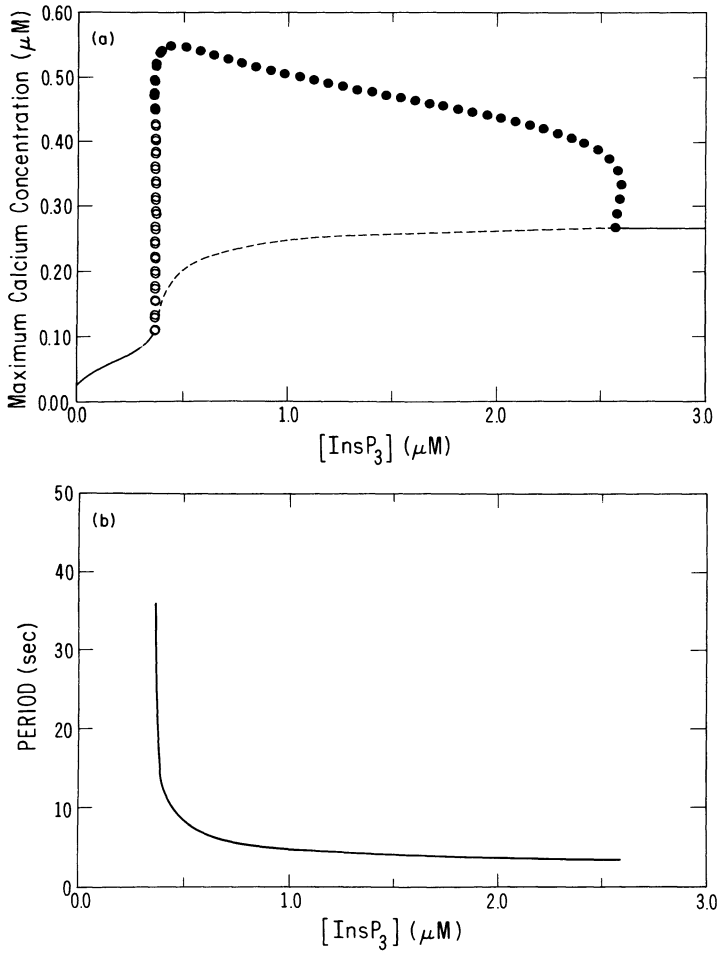

Figure 25.7. (a) The amplitude at steady state (solid and dashed lines) and the maximum amplitude of a periodic solution (open and filled circles) of calcium as a function of the $InsP_3$ concentration. Solid lines and circles indicate stable solutions; dashed lines and open circles indicate unstable solutions. (b) The period in seconds of the periodic solutions in (a). These results were obtained using the software package AUTO (Doedel 1986).

$$\begin{aligned} \frac{dx_2}{dt} &= -k_1 I x_2 + k_{-1} x_3 \\ \frac{dx_3}{dt} &= -(k_{-1} + k_2 x_1) x_3 + k_1 I x_2 + k_{-2} x_4 \\ \frac{dx_4}{dt} &= k_{-3} - k_{-3} x_2 + (k_2 x_1 - k_{-3}) x_3 - (k_{-2} + k_3 x_1 + k_{-3}) x_4. \end{aligned} \tag{25.17}$$

Here y is the dimensionless concentration of $InsP_3$, Δ denotes the Laplace operator, D_{CA} and D_I are the diffusion coefficients of calcium and $InsP_3$, respectively, and H is the dimensionless hormone concentration. Note that we have augmented the previous equations (25.7) to incorporate source terms of $InsP_3$ and first-order decay. In a spatially-uniform system $InsP_3$ relaxes exponentially to the value H. We can thereby mimic experiments in which there

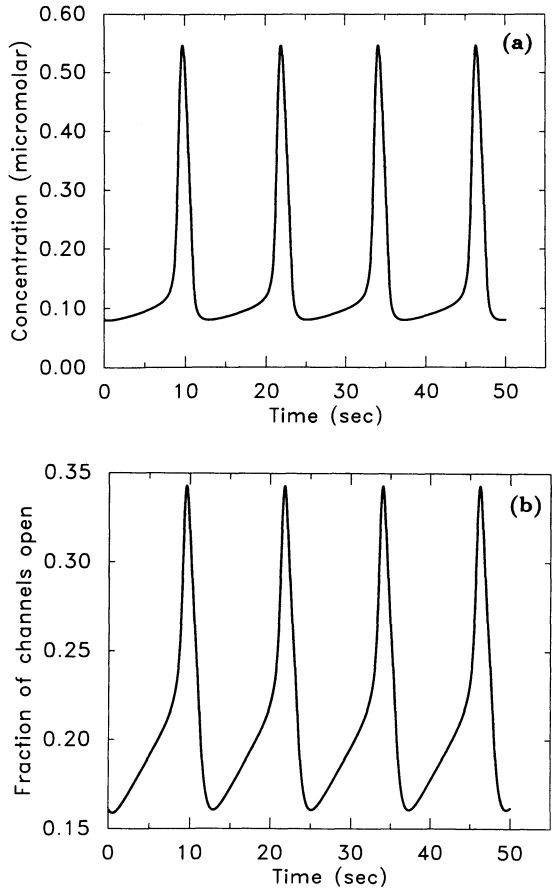

Figure 25.8. The time course of the calcium concentration (a) and the fraction of conducting channels (b) for the periodic solution at $I = 0.4$.

are spatially-distributed sources of $InsP_3$ by specifying the spatial variation of H. We shall describe the solutions of these equations for one- and two-dimensional domains, and for a variety of source distributions. In all cases we impose homogeneous Neumann (*i. e.* zero-flux) boundary conditions on the boundary of the domain. The numerical procedure used is based on a fully-implicit time-stepping algorithm and finite difference approximations to the spatial derivatives. Unless otherwise stated, we use the value $5. \times 10^{-4}\ mm^2/sec$ for both D_{CA} and D_I, and the spatial extent of all systems is 1 mm.

We first solve these equations in a one-dimensional domain. In Figure 25.10 we show the contour lines for waves that originate at a pacemaker located at the center of the domain (by a pacemaker region we mean that if $InsP_3$ in the equations for a spatially-uniform system is fixed at the specified H, then the dynamics in that system would be oscillatory). In Figure 25.10(a) the period of the pacemaker is approximately 12.2 seconds, and 1:1 locking with a period of 14.4 seconds results. The speed of the resulting waves is approximately 16.5 μ/sec, which is in the experimentally-observed range for various systems. However, much more complex patterns result when the pacemaker region has a shorter period, particularly when several pacemakers interact. In Figure 25.10(b) we set

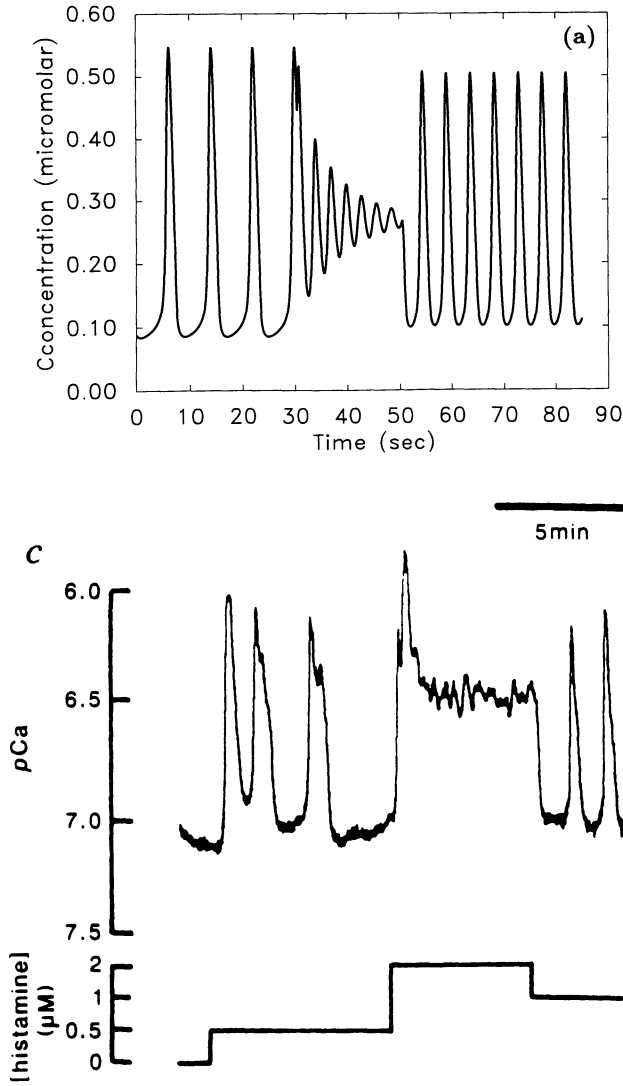

Figure 25.9. (a) The theoretically-predicted calcium concentration, and (b) the experimentally-observed results for endothelial cells. In (a) the $InsP_3$ concentration is held at 0.5 for $T \in (3, 30)$, then is increased to $InsP_3 = 5.$ for 20 seconds, and held at $InsP_3 = 1$ thereafter.

$H = 0.5$ near $x = 0.25$, which gives rise to a period of approximately 8 seconds, and $H = 1.0$ near $x = 0.5$, which produces a period of approximately 4.6 seconds. Note that every other wave that emanates from $x = 0.25$ is blocked, whereas only 2 of every 5 waves that emanate from $x = 0.5$ propagate. What is noteworthy here is that the faster pacemaker does not entrain the slower one; they coexist stably for as long as we have continued the computations.

A similar phenomenon exists in higher dimensions. In Figure 25.11 we show two snapshots of the contour pattern generated by three interacting pacemakers. In this figure $H = 0.4$ within a disk of radius 0.0707 centered at $(0.5, 0.75)$, $H = 1.0$ within a disk of

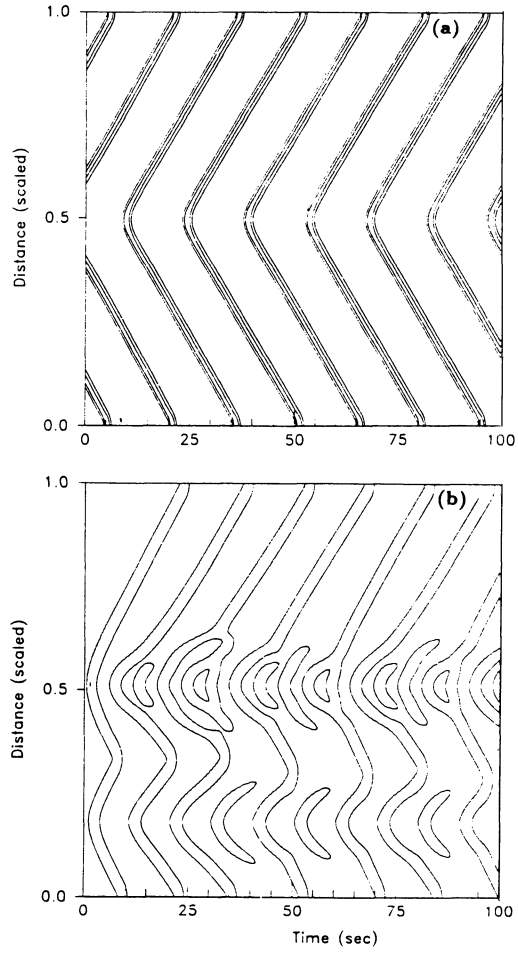

Figure 25.10. (a) The contour lines for waves generated by a pacemaker at the center of the domain ($H = 0.4$ for $x \in (.475, .525)$). (b) The wave patterns when two pacemakers interact. In both (a) and (b) $H = 0.36$ outside the pacemaker regions.

radius 0.0707 centered at $(0.25, 0.25)$, and $H = 1.5$ within a disk of radius 0.0707 centered at $(0.5, 0.25)$ (the last of these produces a period of approximately 3.95 seconds). Again the conclusion is similar to that in one space dimension; pacemakers of widely-disparate periods can coexist stably, apparently indefinitely. In the two-dimensional system we have not established that the overall pattern is in fact periodic.

Other types of waves are also possible. In Figure 25.12 we show a spiral wave that exists when $H = 0.36$ throughout the medium. By examining a sequence of time snapshots of the wave, one finds that the period is approximately 14.9 seconds and the wavelength is 260 μ, which yields a speed of 17.45 μ/sec. Just as multiple pacemakers can coexist stably, so too can a spiral and a pacemaker. In Figure 25.13 we show two time snapshots that illustrate this coexistence. In this figure $H = 0.5$ in a disk of radius 0.0707 centered at $(0.5, 0.5)$, and $H = 0.35$ elsewhere. The coexistence of these waves is more sensitive to parameter values than the multiple pacemakers. If one slightly alters the combination of H values either the pacemaker or the spiral will dominate the asymptotic behavior, depending on the alteration.

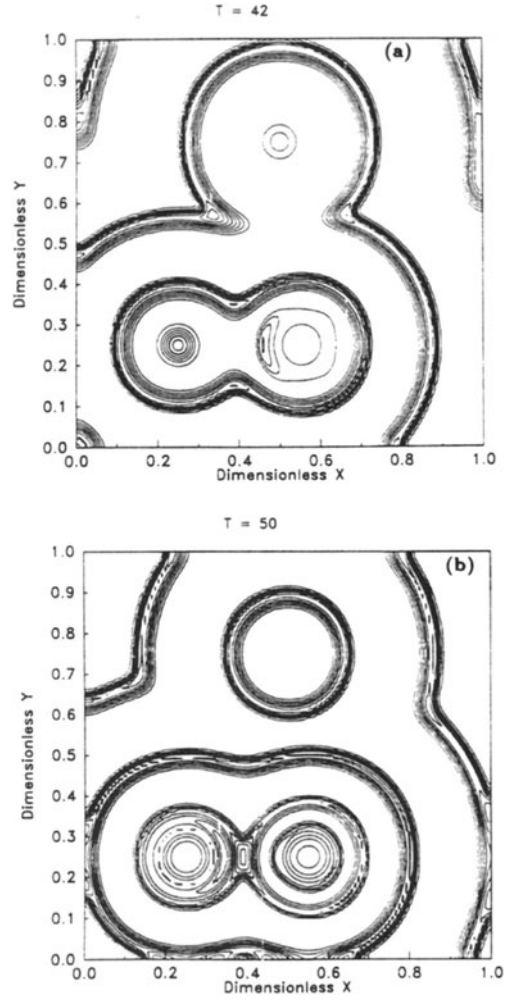

Figure 25.11. The contour pattern of waves produced by three pacemaker regions. $H = 0.36$ outside the pacemaker regions.

However, such solutions are more than a passing curiosity, for they are seen experimentally in oocytes.

25.6 DISCUSSION

As we noted in Section 25.2, there are a number of distinct classes of models for calcium dynamics. Models based on calcium-induced calcium release developed by Berridge and co-workers can reproduce many aspects of the local dynamics, and it has recently been shown that they generate traveling waves (Girard *et al.* 1992; Dupont *et al.* 1991). Similarly, models that involve calcium-activated PLC can also reproduce the observed behavior in some systems. Although it is known that some systems have several types of calcium stores (Brundage *et al.* 1991; Bazotte *et al.* 1991), it is also known that the $InsP_3$-sensitive

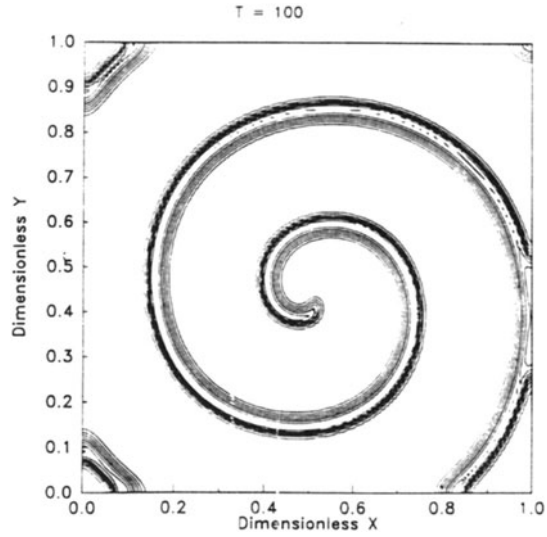

Figure 25.12. A spiral wave propagating through a medium in which $H = 0.36$ everywhere.

store plays an essential role in some systems, and that some systems do not have a calcium-sensitive store (Wakui *et al.* 1989). Within the context of models for a a single $InsP_3$-sensitive pool, one can consider schemes in which $InsP_3$ oscillates and those in which it does not, but oscillation of $InsP_3$ is not essential, as shown by experiments using the non-metabolizable $InsP_3$ analogue $InsP_3S_3$ (Wakui *et al.* 1989). This leads to a model based on one calcium pool with the $InsP_3$ signal as a parameter which controls the various types of response.

The bell-shaped channel opening in response to the calcium levels, which emerges from the four-state model developed here, has been observed in cerebellum cells, using reconstituted membrane containing the channels (Bezprozvanny *et al.* 1991). Moreover, activation of channels at low calcium concentrations and inhibition at high concentrations are seen in a variety of cell types (Zhao *et al.* 1990; Wakui & Petersen 1990; Parker & Ivorra 1990; Meyer & Stryer n.d.). As we have seen, single-pool models based on an $InsP_3$-controlled channel must incorporate more than two states for the $InsP_3$ receptor in order to generate oscillations. This is true even when the activating and inhibitory effects of calcium on the channel dynamics are incorporated. The reason is that the bell-shaped dependence of openings on calcium reflects different time scales, that of the fast activation and that of the slow inhibition, that must be incorporated in the dynamics in order to generate oscillations. The two-state model is too severe a reduction to reflect these scales.

A multi-state model for the $InsP_3$ receptor has been developed by DeYoung and Keizer (1992; 1992). Our model differs from theirs in the following respects: (i) The 4-state model can be studied analytically to understand the origin of the excitable and oscillatory behavior, whereas this is not possible in the 8-state model they propose. (ii) In the DeYoung-Keizer model a channel is assumed to be open only if three subunits in the channel are in the state RIC^+, whereas we assume that a channel can conduct with only one subunit in this state. This implies that the channel in our model can open to 4 different levels, while in theirs it can only open to one level. A major advantage of our four-state model is that we can obtain the bell-shaped distribution directly, and thus show that it arises naturally when there are sequential activation and inhibition calcium binding steps. Moreover, parametric analysis is relatively easy, and the effects of changing on– and off–rates are easy to predict.

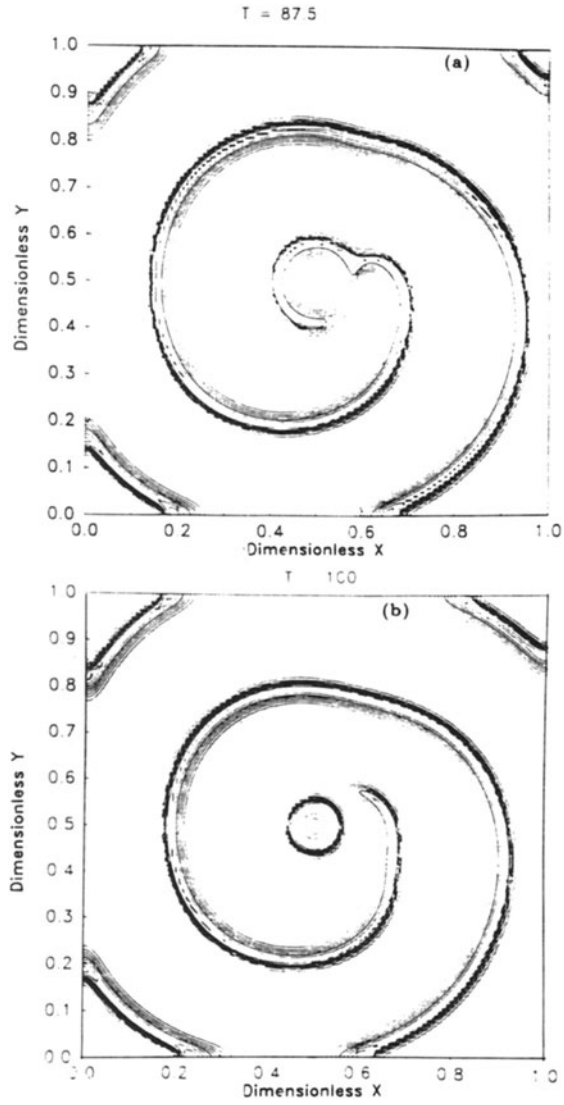

Figure 25.13. The stable coexistence of a spiral and a pacemaker.

The local dynamics of our model show four different types of response to different levels of $InsP_3$ concentrations, namely; a subthreshold response, an excitable response, an oscillatory response with frequency coding, and the over-saturated response. Our model can generate either an oscillatory or an overdamped approach to a high calcium level, depending on the parameters. The second type of response is observed in experiments when $InsP_3$ is very high. The parameter values we used in this paper do not show this type of response, but it is possible with another set of parameters. The different types of responses cover essentially all the local aspects of calcium dynamics observed to date. The distributed versions of our model show traveling waves in one spatial dimension, and target patterns and spiral waves in two spatial dimensions. The new types of wave interaction patterns predicted from numerical calculations are confirmed by experimental results.

Further numerical simulations are needed on the fertilization waves in the *Xenopus* oocyte, the sea urchin egg (Swann & Whitaker 1986), and endothelial cell populations (Boitano *et al.* 1992), where the stimuli are localized. By incorporating positive feedback of Ca^{2+} on $InsP_3$ generation in our model, we have shown that spatially-localized hormone stimuli can generate constant amplitude propagating waves. These results will be reported elsewhere.

Exchange of calcium between the cytoplasm and the extracellular medium is not included in our model, but it can easily be incorporated. If it were, the model would predict that the oscillations die out when calcium is removed from the extracellular medium. Similarly, we could include a calcium-sensitive store, and other types of interactions between the subsystems identified in Section 25.2.

ACKNOWLEDGMENTS This research was supported in part under NIH grant #GM29123.

REFERENCES

Alberts, B., Bray, D., Lewis, J., Raff, M., Roberts, K., & Watson, J. D. 1989. *Molecular biology of the cell.* second edn. New York: Garland Publishing, Inc.

Alexander, J. C., Doedel, E. J., & Othmer, H. G. 1990. On the resonance structure in a forced excitable system. *SIAM J. Appl. Math.*, **50**(5), 1373–1418.

Bazotte, R. B., Pereira, B., Higham, V. Shoshan-Barmatz S., & Kraus-Friedmann, N. 1991. Effects of ryanodine on calcium sequestration in the rat liver. *Biochemical Pharmocology*, **42**(9), 1799–1803.

Berridge, M. J. 1990. Inositol 1,4,5-trisphosphate-induced calcium mobilization is localized in *Xenopus* oocytes. *Proc. Roy. Soc. B*, **238**, 235–343.

Bezprozvanny, I., Watras, J., & Ehrlich, B. E. 1991. Bell-shaped calcium-response curves of $Ins(1,4,5)P_3$- and calcium-gated channels from endoplasmic recticulum of cerebellum. *Nature*, **351**, 751–754.

Boitano, Scott, Dirksen, Ellen R., & Sanderson, Michael J. 1992. Intercellular propagation of calcium waves mediated by inositol trisphosphate. *Science*, **258**(Oct.), 292–295.

Brundage, Rodney A., Fogarty, Kevin E., Tuft, Richard A., & Fay, Fredric S. 1991. Calcium gradients underlying polarization and chemotaxis of eosinophils. *Science*, **254**(Nov.), 703–706.

Cobbold, P. H., Sanchez-Bueno, A., & Dixon, C. J. 1991. The hepatocyte calcium oscillator. *Cell Calcium*, **12**, 87–95.

Cuthbertson, K. S. R., & Chay, T. R. 1991. Modelling receptor-controlled intracellular calcium oscillations. *Cell Calcium*, **12**, 97–109.

De Young, G., & Keizer, J. 1992. A single-pool inositol 1,4,5-trisphophate-receptor-based model for agonist-stimulated oscillations in Ca^{+2} concentration. *Proc. Nat. Acad. Sci.*, **89**, 9895–9899.

Delisle, S. 1991. The four dimensions of calcium signalling in *Xenopus* oocytes. *Cell Calcium*, **12**, 217–227.

DeLisle, S., Krause, K. H., Denning, G., Potter, B. V. L., & Welsh, M. J. 1990. Effect of inositol trisphosphate and calcium on oscillating elevations of intracellular calcium in *Xenopus* oocytes. *J. Biol. Chem.*, **265**, 11726–11730.

Doedel, E. 1986. *AUTO: Software for continuation and bifurcation problems in ordinary differential equations*. Tech. rept. California Institute of Technology.

Dupont, G., Berridge, M. J., & Goldbeter, A. 1991. Signal-induced Ca^{2+} oscillations: Properties of a model based on Ca^{2+}-induced Ca^{2+} release. *Cell Calcium*, **12**, 73–85.

Finch, E. A., Turner, T. J., & Goldin, S. M. 1991. Calcium as a coagonist of inositol 1,4,5-triphosphate-induced calcium release. *Science*, **252**, 443–446.

Gilkey, J. C., Jaffe, L. F., Ridgeway, E. B., & Reynolds, G. T. 1978. A free calcium wave traverses the activating egg of the medaka, *Oryzias latipes*. *J. Cell Biol.*, **76**, 448–466.

Girard, S., Luckhoff, A., Lechleiter, J., Sneyd, J., & Clapham, D. 1992. Two-dimensional model of calcium waves reproduces the patterns observed *Xenopus* oocytes. *Biophys. J.*, **61**, 509–517.

Goldbeter, A., Dupont, G., & Berridge, M. J. 1990. Minimal model for signal-induced Ca^{2+} oscillations and for their frequency encoding through protein phosphorylation. *Proc. Natl. Acad. Sci. USA*, **87**, 1461–1465.

Harootunian, A. T., Kao, J. P. Y., Paranjape, S., & Tsien, R. Y. 1991. Generation of calcium oscillations in fibroblasts by positive feedback between calcium and IP_3. *Science*, **251**, 75–78.

Joseph, S. K., Rice, H. L., & Williamson, J. R. 1989. The effect of external calcium and pH on inositol trisphosphate-mediated calcium release from cerebellum microsomal fraction. *Biochem. J.*, **258**, 261–265.

Keizer, J., & De Young, G. W. 1992. Two roles for Ca^{2+} in agonist stimulated Ca^{2+} oscillations. *Biophys. J.*, pp. 649–660.

Kuba, K., & Takeshita., S. 1981. Simulation of intracellular Ca^{2+} oscillations in a sympathetic neurone. *J. of Theor. Biol.*, **93**, 1009–1031.

Lechleiter, J., & Clapham, D. 1992. Molecular mechanisms of intracellular calcium excitability in *X. laevis* oocytes. *Cell*, **69**, 283–294.

Lechleiter, J., Girard, S., Peralta, E., & Clapham, D. 1991. Spiral calcium wave propagation and annihilation in *Xenopus laevis* oocytes. *Science*, **252**, 123–126.

Lupu-Meiri, M., Shapira, H., & Oron, Y. 1988. Hemispheric asymmetry of rapid chloride responses to inositol trisphosphate and calcium in *Xenopus* oocytes. *FEBS Letts.*, **240**, 83–87.

Meyer, T., & Stryer, L. Transient calcium release induced by successive increments of inositol 1,4,5-trisphosphate. *Proc. Nat. Acad. Sci. USA*.

Meyer, T., & Stryer, L. 1988. Molecular model for receptor-stimulated calcium spiking. *Proc. Natl. Acad. Sci. USA*, **85**, 5051–5055.

Meyer, Tobias. 1991. Cell signaling by second messenger waves. *Cell*, **64**, 675–678.

Meyer, Tobias, & Stryer, Lubert. 1991. Calcium spiking. *Ann. Rev. Biophys. Biophys. Chem.*, **20**, 153–174.

Miyazaki, S., Yuzaki, M., Nakada, K., Shirakawa, H., Nakanishi, S., Nakade, S., & hiba, K. Mikos. 1992. Block of Ca^{2+} wave and Ca^{2+} oscillation by antibody to the inositol 1,4,5-trisphosphate receptor in fertilized hamster eggs. *Science*, **257**, 251–255.

Nuccitelli, R. 1991. How do sperm activate eggs? *Curr. Top. Dev. Biol.*, **25**, 1–16.

Othmer, H. G. 1991. The dynamics of forced excitable systems. In *Nonlinear Wave Processes in Excitable Media*, Holden, A. V., Markus, M., & Othmer, Hans G. (eds), pp. 213–232. NATO, Plenum Press.

Parker, I., & Ivorra, I. 1990. Inhibition by Ca^{2+} of inositol trisphosphate-mediated Ca^{2+} liberation: A possible mechanism for oscillatory release of Ca^{2+}. *Proc. Natl. Acad. Sci USA*, **87**, 260–264.

R. Jacob, J. E. Merritt, T. J. Hallam, & Rink, T. J. 1988. Repetitive spikes in cytoplasmic calcium evoked by histamine in human endothelial cells. *Nature*, **335**(Sept.), 40–45.

Rooney, Thomas A., Sass, Ellen J., & Thomas, Andrew P. 1989. Characterization of cytosolic calcium oscillations induced by phenylephrine and vasopressin in single fura-2-loaded hepatocytes. *J. Biol. Chem.*, **264**(29), 17131–17141.

Somogyi, R., & Stucki, J. W. 1991. Hormone-induced calcium oscillations in liver cells can be explained by a simple one pool model. *J. Biol. Chem.*, **266**(17), 11068–11077.

Swann, Karl, & Whitaker, Michael. 1986. The part played by inositol trisphosphate and calcium in the propagation of the fertilization wave in sea urchin eggs. *J. Cell Biol.*, **103**(6 Pt. 1), 2333–2342.

Thomas, A. P., Renard, D. C., & Rooney, T. A. 1991. Spatial and temporal organization of calcium signalling in hepatocytes. *Cell Calcium*, **12**, 111–126.

Volpe, P., Alderson-Lang, B. H., & Nickols, G. A. 1990. Regulation of inositol 1,4,5-triphosphate-induced Ca^{2+} release. I. effect of Mg^{2+}. *Am. J. Physiol.*, **258**, C1077–C1085.

Wakui, M., & Petersen, O. H. 1990. Cytoplasmic Ca^{2+} oscillations evoked by acetylcholine or intracellular infusion of inositol trisphosphate or Ca^{2+} can be inhibited by internal Ca^{2+}. *FEBS Lett.*, **263**, 206–208.

Wakui, M., Potter, B. V. L., & Petersen, O. H. 1989. Pulsatile intercellular calcium release does not depend on fluctuations in inositol trisphosphate concentrations. *Nature*, **339**, 317–320.

Watras, J., Bezprozvanny, I, & Ehrlich, B. E. 1991. Inositol 1,4,5-trisphoshate-gated channels in cerebellum: Presence of multiple conductance states. *J. Neuroscience*, **11**(10), 3239–3245.

Wong, Alan Y. K., Fabiato, Alexandre, & Bassingthwaigthe, J. B. 1992. Model of calcium-induced calcium release mechanism in cardiac cells. *Bulletin of Mathematical Biology*, **54**(1), 95–116.

Woods, N. M., Cuthberson, K. S. R., & Cobbold, P. H. 1986. Repetitive transient rises in cytoplasmic free calcium in hormone-stimulated hepatocytes. *Nature*, **319**, 600–602.

Zhao, Hong, Loessberg, Peggy A., Sachs, George, & Muallem, Shmuel. 1990. Regulation of intracellular Ca^{2+} oscillation in AR42J cells. *J. Biol. Chem.*, **265**(34), 20856–20862.